



UNIVERSITY OF LEEDS

This is a repository copy of *σ -Alkenyl endo-palladacycle formation via regiospecific functionalisation of an unreactive NHC-tethered C(sp²)-H bond*.

White Rose Research Online URL for this paper:
<http://eprints.whiterose.ac.uk/84072/>

Version: Accepted Version

Article:

Chapman, MR, Pask, CM, Ariafard, A et al. (1 more author) (2015) σ -Alkenyl endo-palladacycle formation via regiospecific functionalisation of an unreactive NHC-tethered C(sp²)-H bond. *Chemical Communications*, 51 (25). 5513 - 5515. ISSN 1359-7345

<https://doi.org/10.1039/c4cc10163d>

Reuse

Items deposited in White Rose Research Online are protected by copyright, with all rights reserved unless indicated otherwise. They may be downloaded and/or printed for private study, or other acts as permitted by national copyright laws. The publisher or other rights holders may allow further reproduction and re-use of the full text version. This is indicated by the licence information on the White Rose Research Online record for the item.

Takedown

If you consider content in White Rose Research Online to be in breach of UK law, please notify us by emailing eprints@whiterose.ac.uk including the URL of the record and the reason for the withdrawal request.



eprints@whiterose.ac.uk
<https://eprints.whiterose.ac.uk/>

COMMUNICATION

σ -Alkenyl endo-palladacycle formation via regioselective functionalisation of an unreactive NHC-tethered C(sp²)–H bond

Cite this: DOI: 10.1039/x0xx00000x

Received 00th January 2012,
Accepted 00th January 2012Michael R. Chapman,^a Christopher M. Pask,^a Alireza Ariafard^{b*} and Charlotte E. Willans^{a*}

DOI: 10.1039/x0xx00000x

www.rsc.org/

An unusual cyclometallation reaction at palladium is described, which proceeds via C–H functionalisation of a vinylic C(sp²)–H bond tethered to an NHC ligand. The energetic balance between palladacycle formation and bis-NHC complexation has been found to be very subtle.

Metallacycles are ubiquitous in catalytic transformations, featuring as transient reactive intermediates in a variety of metal-mediated cycles, whilst concomitantly holding a firm position as structurally defined pre-catalysts themselves.^{1, 2} Pioneered by Herrmann and co-workers in 1995,³ palladacyclic complexes have showcased extensive utility in prolific catalytic processes such as C–C cross-coupling^{4, 5} and allylic substitution,⁶ and have more recently emerged as promising antimicrobial agents.⁷ Traditional routes to palladacyclic scaffolds involve a metal-induced C–H activation process paralleled by coordination of pendant heteroatom donors (e.g. imines,⁸ amines,⁹ phosphines,¹⁰ oximes,¹¹ thioethers¹² and oxazolines¹³) to the metal centre. The absolute position of the C–H bond to be activated with respect to the donor atom(s), in conjunction with the degree of hybridisation of the related carbon atom, bear significant influence on the ease of cyclometallation. In light of such governing parameters, the majority of cyclometallated complexes are restricted to form via C(sp²)–H activation at an aromatic carbon (Figure 1 A), or C(sp³)–H activation at an aliphatic or benzylic carbon atom (Figure 1 B).^{14, 15}

Whilst C(sp³)–H activation is a rapidly expanding field of research, the direct activation of non-acidic, non-aromatic sp²-hybridised C–H bonds is far less explored. Investigations in our laboratory focus on the reactivity and applications of N-heterocyclic carbenes (NHCs) as ancillary ligands for a broad scope of chemical transformations. Despite occasional union throughout the last decade, NHCs have seldom been employed as supporting ligands for Pd metallacycles, and typical syntheses require coordination of a free carbene to a pre-

existing palladacyclic framework (Figure 1 C)¹⁶ or oxidative addition to Pd⁰ of a heteroaryl precursor (Figure 1 D).¹⁷

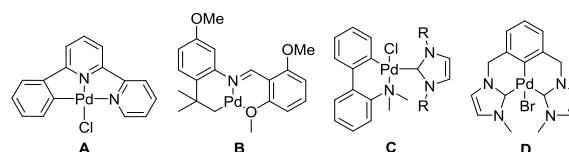
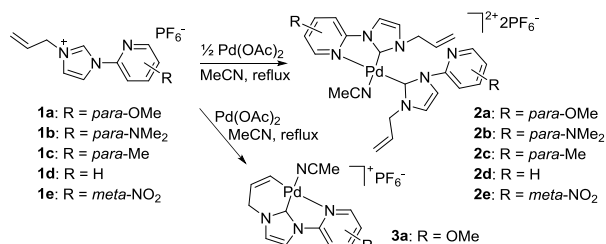


Figure 1 Representative palladacycles formed via aromatic C(sp²)–H or C(sp²)–X activation (A, C, D) and aliphatic C(sp³)–H activation (B).

In light of the subtle electronic/proximity balance required to activate an unconjugated sp² orbital, selective functionalisation of such unreactive positions remains a challenge. To our knowledge, no NHC-ligated pincer complex which houses a stable σ -alkenyl palladacyclic motif is known. Herein, we report a palladacyclisation via C(sp²)–H activation of a distal vinylic proton appended to an NHC. The cyclometallation proceeds from a pendant terminal alkene to deliver a σ -alkenyl palladacyclic NHC as a single endocyclic regioisomer, with full retention of the C=C double bond.

It has previously been found that pyridyl-appended NHC ligands stabilise variable metal oxidation states, and can be tuned to enhance catalysis.^{18, 19} Two equivalents of pyridyl-appended imidazolium ion **1a** were stirred in refluxing MeCN with Pd(OAc)₂ to deliver the corresponding bis-NHC coordinated Pd^{II} complex **2a** (Scheme 1).



Scheme 1 Synthesis of Pd^{II}-bis-NHC complexes **2a-2e** and palladacycle **3a**.

Single crystals of **2a** suitable for X-ray diffraction analysis were grown via vapour diffusion of Et₂O into an MeCN solution (Figure 2). The two independent NHC moieties in the solid-state structure are orthogonal to one another, with the metal-coordinated pyridyl ligand residing in the plane of the adjacent carbene and the non-coordinated pyridyl group lying perpendicular to the plane of the neighbouring carbene. The geometry around the Pd centre is distorted square planar and the NHC ligands adopt a *cis* configuration. One molecule of solvating MeCN co-crystallises with the complex to satisfy a vacant coordination site; the contracted carbenic/pyridyl bond angle (79.63°) around the Pd appears too strained to allow pyridyl coordination from both ligands. The five-membered C, N-palladacycle assumes a ‘flattened envelope’-like arrangement with an average intrachelate torsion angle of 6.1° which is in line with similar complexes previously reported.²⁰

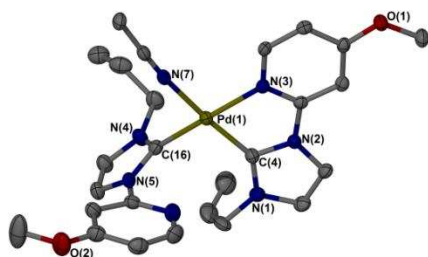


Figure 2 Molecular structure of Pd^{II}-bis-NHC complex **2**. Ellipsoids shown at the 50% probability level, hydrogen atoms and counter anions omitted for clarity.

Subsequent ¹H-¹H COSY NMR spectroscopy and mass spectrometry experiments of the recrystallised reaction mixture containing **2a** also highlighted the formation of another complex. Alongside crystallisation of **2a** arose a collection of pale yellow crystals of plate-like morphology. Therein, it was confirmed that an unusual NHC-ligated pincer complex was formed via cyclometallation of a pendant allyl tether with the Pd centre, delivering endocyclic σ -alkenyl palladacycle **3a**. The 1-allyl-3-(2-(4-methoxy)pyridyl)imidazole-2-ylidene ligand in the solid-state structure of **3a** (Figure 3) is approximately coplanar, coordinating to the metal centre via a tridentate C,C,N pincer interaction to furnish a 5,6-fused palladacycle. The geometry around the Pd centre is distorted square planar. The C(3)-C(2)-C(1)-Pd(1) torsion angle is defined at 28.90°, giving rise to a partially puckered synclinal conformation of the metallated alkene. Interestingly, the C(15)-Pd(2)-N(7) bond angle is 164.2(10)°, deviating vastly from a linear value due to the requirement of pincer-type coordination.

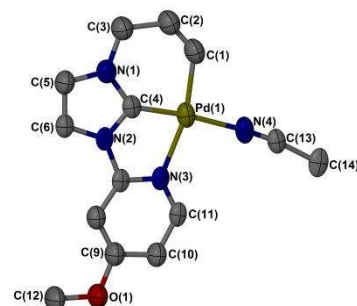


Figure 3 Molecular structure of NHC palladacycle **3a**.[†] Ellipsoids shown at the 30% probability level, hydrogen atoms and counter anions omitted for clarity.

As the pK_a of a vinylic proton far exceeds that of the conjugate acid of acetate, an intramolecular C(sp²)-H activation mechanism is implied for palladacycle formation. With this in mind, a solution of imidazolium salt **1a** (0.03 M) in MeCN was added dropwise to a stirred solution of Pd(OAc)₂ (0.11 M) in uniform solvent at 80 °C to maintain control via a high dilution strategy. Therein, σ -alkenyl endo-palladacycle **3a** was formed exclusively, with competitive bis-NHC complex **2a** being spectroscopically undetectable. The observed results support an intramolecular mechanism, as reducing the effective concentration of imidazolium **1a** with respect to Pd allows irreversible formation of a single mono-NHC ligated product. An identical reaction using the imidazolium hexafluoroantimonate salt also yielded a palladacycle with similar spectroscopic and crystallographic data (see ESI). Surprisingly however, modifying the electronic properties of the pyridyl substituent (imidazolium salts **1b-1e**) yielded only bis-NHC complexes **2b-2e**, with no evidence of palladacycle formation under identical high dilution conditions (see ESI). This indicates that the ligand bearing a *para*-methoxypyridyl substituent is a unique case in palladacycle formation, and that an extremely fine electronic balance is required to promote C(sp²)-H activation.

Density functional theory (DFT) calculations were performed in an attempt to rationalise the apparent fine balance between C-H proximity and metal electronics. Initially, the deprotonation of the first imidazolium NCHN proton was considered (Figure 4 and Figure S6 in ESI). The DFT calculations illustrate that the most stable palladium acetate adduct in MeCN exists as a square planar *cis*-MeCN complex (**4**). As imidazolium **1** is introduced, the ligand initially binds via the pyridyl nitrogen atom to Pd (**8**). Latterly, deprotonation occurs via an unexpected trigonal bipyramidal transition state structure (**ITS**), whereby a coordinated MeCN molecule lowers the activation energy. To our knowledge, a five-coordinate Pd transition structure is unprecedented, and is in vast contrast to the traditional mechanism transition state currently theorised in the literature.²¹⁻²³ The four-coordinate transition state is favoured in the absence of MeCN (2TS vs. 3TS in ESI), however, these studies indicate that a five-coordinate transition structure may be more general in the presence of strong coordinating solvents.

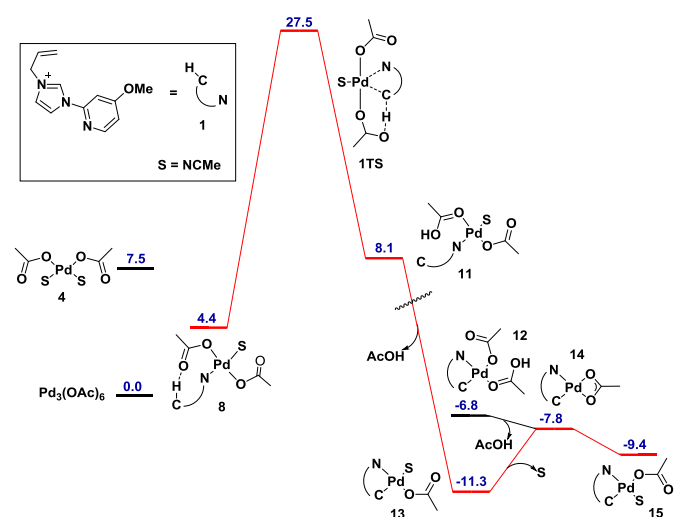


Figure 4 DFT investigations into imidazolium deprotonation. ΔG values are calculated in kcalmol^{-1} . See ESI for energies of alternative pathways. Palladium complexes **11–15** are cationic.

Further, the origin of palladacyclisation was evaluated against competitive bis-NHC complexation. The initial calculation predicts that the reaction between palladium acetate and one equivalent of imidazolium **1** is exergonic (Figure 4), with the most stable intermediate being **13**. However, DFT calculations indicate that addition of the second equivalent of **1** occurs at **15**, as the activation energy is less favourable starting from **13** (see ESI). The two reaction pathways for palladacyclisation and bis-NHC complexation were found to be remarkably close in energetic penalties, with only 0.9 kcalmol^{-1} difference in free energy barriers (**4TS** and **5TS**) (Figure 5). It is also notable that the two pathways are not exceedingly exergonic, which is attributed to steric factors as evidenced by a distorted square planar geometry in complex **2**. The formation of the bis-NHC Pd^{II} complex is calculated to be thermodynamically favoured over palladacyclisation, with the transition structure (**5TS**) also displaying the unusual five-coordinate trigonal bipyramidal coordination geometry. These calculations are very much level with experimental findings, as controlling reaction stoichiometry and order of addition enables selective formation of either complex. However, DFT calculations are unable to provide an explanation for the absence of palladacycle formation under kinetic control when the para-methoxypyridyl substituent is exchanged for varying pyridyl substituents (i.e. imidazolium salts **1b–1e**). Calculations show that the energies of the palladacycle and bis-NHC in each case are comparable, as are the activation barriers (see ESI). This discrepancy may be related to error in the calculation,[‡] or an unknown reaction condition that switches off palladacyclisation in favour of bis-NHC formation.

Interestingly, according to DFT calculations, addition of the first NHC ($27.5 \text{ kcalmol}^{-1}$) is calculated to be much slower than addition of the second NHC ($23.4 \text{ kcalmol}^{-1}$), as the particularly stable $\text{Pd}_3(\text{OAc})_6$ renders the first step highly energy consuming. The first addition being the rate-determining step is

consistent with experimental findings, as the mono-NHC Pd complex (**13** or **15**) is never observed spectroscopically. The DFT model also predicts that cyclometallation should be sequestered in different reaction media, as solvating MeCN reduces the energy price associated with cyclisation. Attempts to form the palladacycle in THF, DMSO and DMF were unsuccessful, with only bis-NHC Pd^{II} complex (**2a**) being observed.

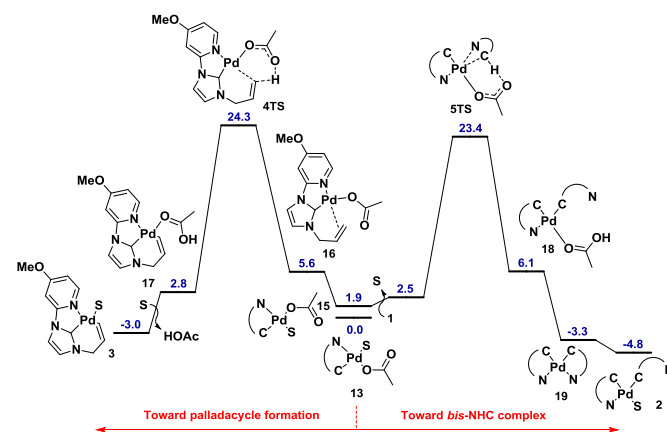


Figure 5 DFT analysis of competitive energy pathways for palladacyclisation versus bis-NHC formation. ΔG values are calculated in kcalmol^{-1} . Palladium complexes are cationic.

Conclusions

Palladacycle formation via aliphatic vinylic $\text{C}(\text{sp}^2)\text{-H}$ activation has been found to compete with bis-NHC Pd^{II} complexation. A fine energetic difference between the two pathways enables the selective synthesis of either complex through tuning the pyridyl substituent and reaction stoichiometry. We have uncovered non-linear substituent effects in pyridyl systems which is essential to report, as subtle changes in pyridyl electronics often leads to unusual/unexpected behaviour in catalysis (e.g. in Organ's PEPPSI precatalysts).²⁴ Furthermore, an unprecedented five-coordinate Pd transition structure is favoured upon deprotonation of each imidazolium moiety in the presence of a coordinating solvent.

Notes and references

^a School of Chemistry, University of Leeds, Woodhouse Lane, Leeds, LS2 9JT, UK.

^b School of Chemistry, University of Tasmania, Private Bag 75, Hobart, Tasmania 7001, Australia. Department of Chemistry, Faculty of Science, Central Tehran Branch, Islamic Azad University, Shahrak Gharb, Tehran, Iran.

[†] Structure solutions of both the PF_6 and SbF_6 salts of palladacycle **3** gave similar molecular structures which were entirely consistent with other experimental and theoretical data. Both sets of crystals diffracted poorly at high angles and the SbF_6 salt showed extensive twinning, leading to higher than normal residual values. We would like to thank Prof. Michael Hardie for help and advice on structure refinements.

- ‡ The error can be related to the estimation of entropy effects. The formulation developed by Whitesides and co-workers²⁵ was used to reduce the error which, in some cases, may be underestimated (see ESI). Electronic Supplementary Information (ESI) available: Experimental, crystallographic and computational details. See DOI: 10.1039/c000000x/
1. I. P. Beletskaya and A. V. Cheprakov, *J. Organomet. Chem.*, 2004, **689**, 4055-4082.
 2. G. R. Peh, E. A. B. Kantchev, J. C. Er and J. Y. Ying, *Chem.-Eur. J.*, 2010, **16**, 4010-4017.
 3. W. A. Herrmann, C. Brossmer, K. Ofele, C. P. Reisinger, T. Priermeier, M. Beller and H. Fischer, *Angew. Chem.-Int. Edit. Engl.*, 1995, **34**, 1844-1848.
 4. W. A. Herrmann, C. Brossmer, C. P. Reisinger, T. H. Riermeier, K. Ofele and M. Beller, *Chem.-Eur. J.*, 1997, **3**, 1357-1364.
 5. W. A. Herrmann, V. P. W. Bohm and C. P. Reisinger, *J. Organomet. Chem.*, 1999, **576**, 23-41.
 6. B. M. Trost and D. L. VanVranken, *Chem. Rev.*, 1996, **96**, 395-422.
 7. A. R. Kapdi and I. J. S. Fairlamb, *Chem. Soc. Rev.*, 2014, **43**, 4751-4777.
 8. J. L. Serrano, L. Garcia, J. Perez, E. Perez, J. Garcia, G. Sanchez, P. Sehnal, S. De Ornellas, T. J. Williams and I. J. S. Fairlamb, *Organometallics*, 2011, **30**, 5095-5109.
 9. Y. Ding, Y. X. Li, Y. Zhang, S. A. Pullarkat and P. H. Leung, *Eur. J. Inorg. Chem.*, 2008, 1880-1891.
 10. G. R. Rosa and D. S. Rosa, *RSC Advances*, 2012, **2**, 5080-5083.
 11. J. F. Civicos, D. A. Alonso and C. Najera, *Eur. J. Org. Chem.*, 2012, 3670-3676.
 12. G. K. Rao, A. Kumar, S. Kumar, U. B. Dupare and A. K. Singh, *Organometallics*, 2013, **32**, 2452-2458.
 13. S. F. Kirsch, L. E. Overman and M. P. Watson, *J. Org. Chem.*, 2004, **69**, 8101-8104.
 14. S. W. Lai, T. C. Cheung, M. C. W. Chan, K. K. Cheung, S. M. Peng and C. M. Che, *Inorg. Chem.*, 2000, **39**, 255-262.
 15. B. D. Dangel, K. Godula, S. W. Youn, B. Sezen and D. Sames, *J. Am. Chem. Soc.*, 2002, **124**, 11856-11857.
 16. O. Navarro, R. A. Kelly and S. P. Nolan, *J. Am. Chem. Soc.*, 2003, **125**, 16194-16195.
 17. S. Grundemann, M. Albrecht, J. A. Loch, J. W. Faller and R. H. Crabtree, *Organometallics*, 2001, **20**, 5485-5488.
 18. B. R. M. Lake and C. E. Willans, *Organometallics*, 2014, **33**, 2027-2038.
 19. V. Khlebnikov, A. Meduri, H. Mueller-Bunz, T. Montini, P. Fornasiero, E. Zangrando, B. Milani and M. Albrecht, *Organometallics*, 2012, **31**, 976-986.
 20. O. N. Gorunova, K. J. Keuseman, B. M. Goebel, N. A. Kataeva, A. V. Churakov, L. G. Kuz'mina, V. V. Dunina and I. P. Smoliakova, *J. Organomet. Chem.*, 2004, **689**, 2382-2394.
 21. M. Anand, R. B. Sunoj and H. F. Schaefer, *J. Am. Chem. Soc.*, 2014, **136**, 5535-5538.
 22. G. J. Cheng, Y. F. Yang, P. Liu, P. Chen, T. Y. Sun, G. Li, X. H. Zhang, K. N. Houk, J. Q. Yu and Y. D. Wu, *J. Am. Chem. Soc.*, 2014, **136**, 894-897.
 23. A. J. Canty, A. Ariafard, M. S. Sanford and B. F. Yates, *Organometallics*, 2013, **32**, 544-555.
 24. C. Valente, M. Pompeo, M. Sayah and M. G. Organ, *Org. Process Res. Dev.*, 2014, **18**, 180-190.
 25. M. Mammen, E. I. Shakhnovich, J. M. Deutch and G. M. Whitesides, *J. Org. Chem.*, 1998, **63**, 3821-3830.